Interpretation of Pioneer 10 Ly- α based on heliospheric interface models: methodology and first results

Pradip Gangopadhyay[1], Vlad Izmodenov[2], Mike Gruntman[1], Darrell Judge[1]

(1) University of Southern California, Los Angeles

(2) Lomonosov Moscow State University, Department of Aeromechanics and Gas Dynamics, Faculty of Mathematics and Mechanics, Moscow, 119899, Russia

Abstract. The Very Local Interstellar Medium (VLISM) neutral hydrogen and proton densities are still not precisely known even after three decades of deep space research and the existence of the EUV and other diagnostic data obtained by Pioneer 10/11, Voyager 1/2 and other spacecraft. The EUV data interpretation, in particular, has suffered because of inadequate neutral hydrogen-plasma models, difficulty of calculating the multiply scattered Lyman α glow and calibration uncertainties. Recently, all these difficulties have been significantly reduced. In the present work we have used the latest state of the art supersonic VLISM neutral hydrogen-plasma and Monte Carlo radiative transfer model, incorporating neutral density, temperature, and velocity variations, actual solar line shape, realistic redistribution function, Doppler and aberration effects. This work presents the methodology of the radiative transfer code and the first results of the comparison of the model predictions with the Pioneer 10 data. Monte Carlo radiative transfer calculations were carried out for five neutral hydrogen- plasma models and compared with Pioneer data. The first results are quite encouraging. We found that the VLISM ionization ratio is between 0.2 and 0.5 and that the VLISM neutral hydrogen density is less than 0.25 cm^{-3}. The present calculation suggests that the Pioneer 10 photometer derived intensities (Rayleighs) need to be increased by a factor of 2. If this model- derived calibration is used then the difference between Pioneer 10 and Voyager 2 intensity values is reduced to about 2.2. The model, neutral hydrogen density=0.15 cm^{-3} and proton density=0.07 cm^{-3}, is found to best fit the Pioneer 10 data.

1. Introduction

The heliospheric interface, formed due to the interaction between the solar wind and the local interstellar cloud (LIC), is a very complicated phenomenon where the solar wind and interstellar plasmas, interstellar neutrals, magnetic field, and cosmic rays play prominent roles [*Axford*, 1972; *Holzer*, 1972]. The heliosphere provides a unique opportunity to study in detail the only accessible example of a commonplace but fundamental astrophysical phenomenon - the formation of an astrosphere. The heliospheric interface is a natural "environment" of our star and knowledge of its characteristics is important for the interpretation and planning of space experiments. In fact, the growing body of evidence about the interface using different sets of data including Lyman α data [*Hall et al.*,1993; *Kurth and Gurnett*, 1993; *Cummings, Stone and Webber*, 1993; *Linsky and Wood*, 1996; *Gloeckler and Geiss*, 2001; *Wang and Richardson*, 2001] shows that the properties of the neutral hydrogen distribution are significantly affected by processes in the interface between the interstellar medium and the solar wind and that a 'no interface model' can not explain the observations. Thus it is specially important to include the effect of the interface in the interpretation of deep space spacecraft data. In this work we have included the effect of the interface in the interpretation of the Pioneer 10 photometer hydrogen channel data.

Paper number 2002???00021.
0148-0227/02/2002???00021$9.00

Remote sensing of the heliospheric interface through the study of the interstellar hydrogen atoms is possible since H atoms play a very important role in the formation of the heliospheric interface. Interstellar H atoms are strongly coupled with plasma protons by charge exchange. The charge exchange process leads to a significantly smaller heliosphere. The interstellar neutral hydrogen atoms penetrate deeply into the heliosphere since the mean free path is comparable to the size of the heliosphere. Inside the heliosphere, the atoms and their derivatives such as pickup ions and anomalous cosmic rays are measured. These species become major sources of observational information on the heliospheric interface and therefore on the local interstellar medium properties. For example, direct detection of the flux of the interstellar neutral helium allows the determination of the Sun/LIC relative velocity and local interstellar temperature [*Witte et al.*, 1993, 1996]. Interstellar helium atoms are not affected by the heliospheric interface plasma due to their small charge exchange cross section with protons. In contrast to helium, interstellar hydrogen atoms have strong coupling with heliospheric plasma protons. Distribution of these atoms inside the heliosphere has imprints of the heliospheric interface. Thus, interstellar hydrogen atoms provide excellent remote diagnostics on the structure of the heliospheric interface.

The study of the neutral hydrogen atoms in the outer heliosphere has been made possible by the presence of four deep space spacecraft, Pioneers 10 and 11 (P10 and P11), and Voyagers 1 and 2 (V1 and V2). The USC photometers on-board P10 and P11 and the ultraviolet spectrometers (UVS) on-board V1 and V2 have measured the interplanetary Ly α background radiation for more than twenty years. Various studies of P10/11 and V1/2 Ly α data have been published [*Wu et. al.*, 1981, 1988; *Shemansky et al.*, 1984; *Ajello et al.*,

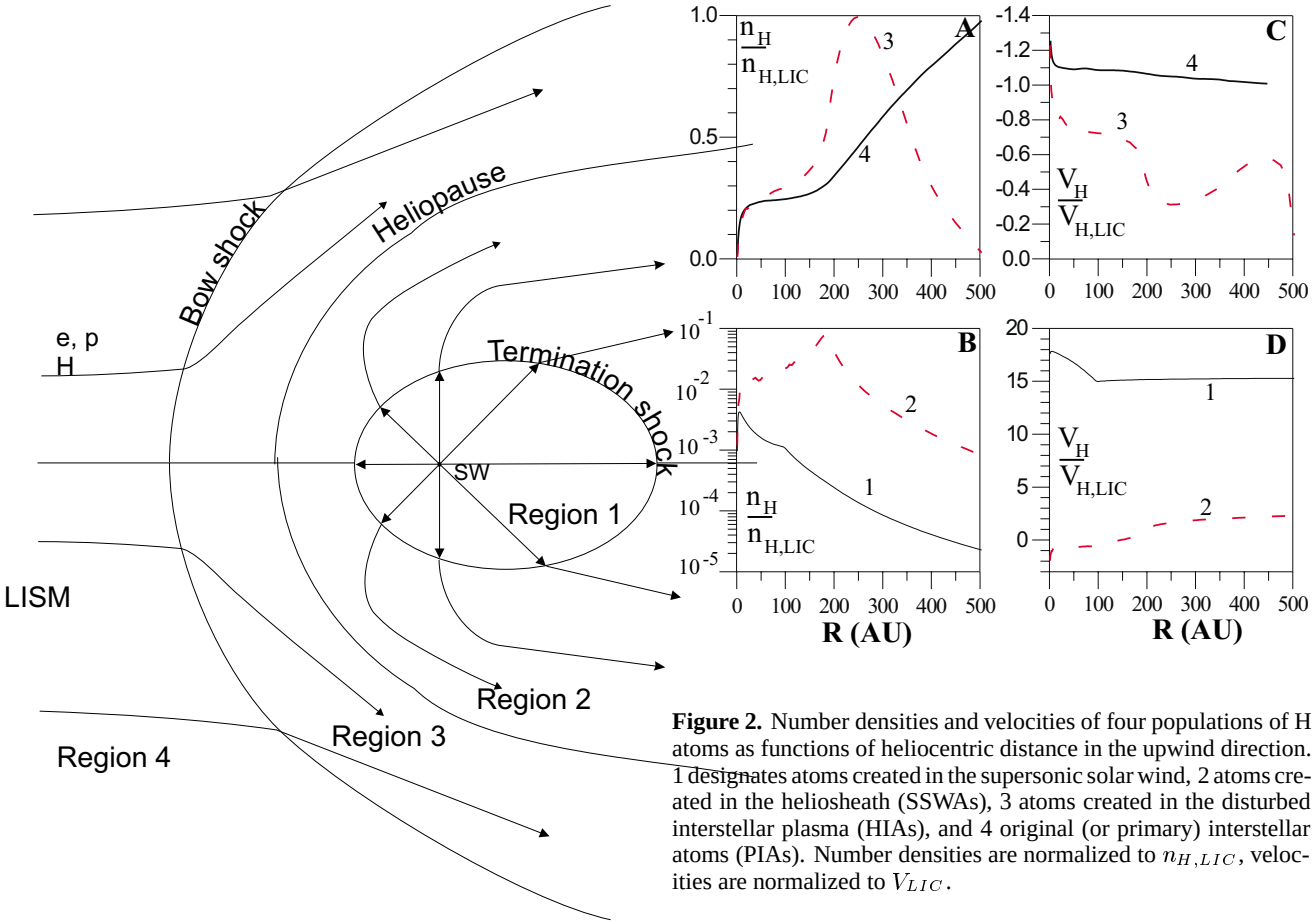

Figure 2. Number densities and velocities of four populations of H atoms as functions of heliocentric distance in the upwind direction. 1 designates atoms created in the supersonic solar wind, 2 atoms created in the heliosheath (SSWAs), 3 atoms created in the disturbed interstellar plasma (HIAs), and 4 original (or primary) interstellar atoms (PIAs). Number densities are normalized to $n_{H,LIC}$, velocities are normalized to V_{LIC}.

Figure 1. The heliospheric interface is the region of the solar wind interaction with LIC. The heliopause is a contact discontinuity, which separates the plasma wind from interstellar plasmas. The termination shock decelerates the supersonic solar wind. The bow shock may also exist in the interstellar medium. The heliospheric interface can be divided into four regions with significantly different plasma properties: 1) supersonic solar wind; 2) subsonic solar wind in the region between the heliopause and termination shock; 3) disturbed interstellar plasma region (or "pile-up" region) around the heliopause; 4) undisturbed interstellar medium.

1987; *Gangopadhyay et al.*, 1989; *Hall et al.*, 1993; Quémerais et al., 1995,1996; Gangopadhyay and Judge, 1995, 1996]. Yet, the estimation of the interstellar H atom density varies greatly from study to study, ranging between 0.03 and 0.3 cm-3 [see, *Quemerais et al.*, 1994].

Hall et al. [1993] found that the Ly α intensity falls with heliocentric distance less quickly than expected from a standard hot model. This result suggested that there was a positive gradient of H atom density at large distances from the Sun. This can be explained by a hydrogen wall around the heliosphere confirmed by *Lallement et al.* [1993]. However, *Quemerais et al.* [1995] suggested an alternative explanation. The latter work suggested that the increase of Ly α intensity in the upwind direction could be partially due to the constant emission from HII regions in the galactic plane.

The study of the heliosphere has been made more difficult by the calibration difference of 4.4 at Lyman α between the V1/2 spectrometers and P10/11 photometers found by *Shemansky et al.* [1984]. This difference was determined by comparing V2 and P10 data when both spacecraft looked in the same direction and at the same time. Finally, the picture is further complicated by the change in the absolute value of the solar Ly α flux since 1993. Recently, past solar Lyman α irradiance measurements have been consolidated into a long-term composite time series [Woods and Rottman, 1997; Tobiska et al. 1997; Woods et al., 2000]. This was done by adjusting Atmospheric Explorer E (AE-E) and the Solar Mesospheric Explorer (SME) to agree with the Upper Atmospheric Research Satellite (UARS) Solar Stellar Irradiance Comparison Experiment (SOLSTICE) data. This resulted in changes in reported solar Lyman α measurements obtained by both the SME and the AE-E satellites. Of course, the calculation reported here assumes that the line center flux varies the same way as the total flux. If this assumption does not hold then that will introduce an additional uncertainty.

In this paper we will describe the methodology and the first results of our reanalysis of the P10 Ly α data to improve our knowledge of the very local interstellar neutral hydrogen and proton densities. This reanalysis uses the latest state of the art neutral hydrogen-plasma and radiative transfer models outlined in the later sections.

2. Model of the H atom distribution

The interaction of the solar wind with the interstellar medium influences the distribution of interstellar atoms inside the heliosphere. Further, it is now clear that the Local Interstellar Cloud is partly ionized and that the plasma component of the LIC interacts with the solar wind plasma to form the heliospheric interface (Figure 1). Interstellar H atoms interact with the plasma component through charge exchange. This interaction strongly influences both the plasma and neutral components. The main difficulty in the modeling of the H atom flow in the heliospheric interface is its kinetic character due to the large, i.e. comparable to the size of the

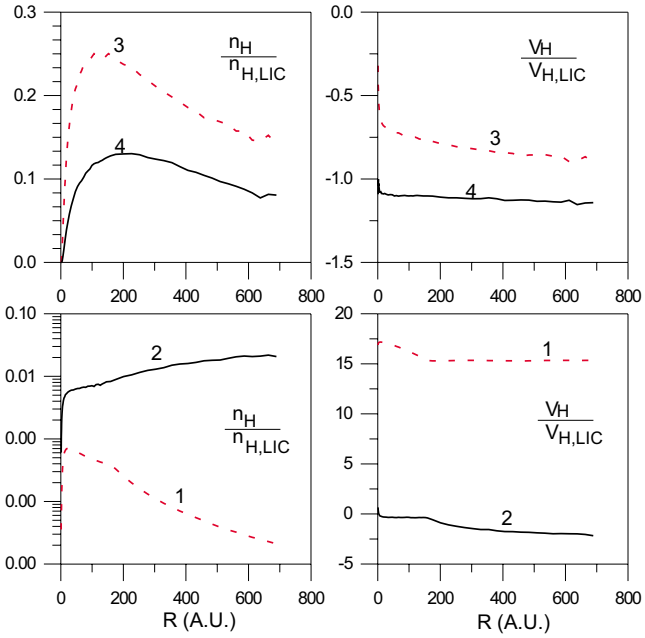

Figure 3. Number densities and velocities of four populations of H atoms as functions of heliocentric distance in the downwind direction. Notations are the same as in figure 2.

interface, mean free path of H atoms with respect to the mean free path for charge exchange process. In this paper to get the H atom distribution in the heliosphere and heliospheric interface structure, we use the self-consistent model developed by Baranov and Malama [1993]. The kinetic equation for the neutral component and the hydrodynamic Euler equations were solved self-consistently by the method of global interactions. To solve the kinetic equation for H atoms, an advanced Monte Carlo method with splitting of trajectories [*Malama*, 1991] was used. Basic results of the model were reported by *Baranov and Malama* [1995], *Izmodenov et al.* [1999], *Izmodenov* [2000], and *Izmodenov et al.* [2001].

Hydrogen atoms newly created by charge exchange have the velocities of their ion partners in charge exchange collisions. Therefore, the parameters of these new atoms depend on the local plasma properties. It is convenient to distinguish four different populations of atoms depending on where in the heliospheric interface they originated. Population 1 corresponds to the atoms created in the supersonic solar wind noted as **SSWA** (supersonic solar wind atoms). Population 2 (noted **HSWA**, hot solar wind atoms) represents the atoms originating in the heliosheath and known as heliospheric ENAs [*Gruntman et al.*, 2001]. Population 3 (**HIA**, hot interstellar atoms) consists of the atoms created in the disturbed interstellar wind. We will call original (or primary) interstellar atoms population 4 (**PIA**, primary interstellar atoms). The number densities and mean velocities of these populations are shown in Figures 2 and 3 as functions of the heliocentric distance in the upwind and downwind directions respectively.

The main results of the model for the H atom populations can be summarized as follows:

PIAs are significantly filtered (i.e. their number density is reduced) before reaching the termination shock. Since slow atoms have a smaller mean free path as compared with fast atoms, they undergo more charge exchange. This kinetic effect, called *selection*, results in a deviation of the interstellar distribution function from Maxwellian [*Izmodenov et al.*, 2001]. The selection also results in $\sim$10 % increase of the primary atom mean velocity at the termination shock (Figure 2C).

HIAs are created in the disturbed interstellar medium by charge exchange of primary interstellar neutrals and protons decelerated by the bow shock. The secondary interstellar atoms collectively make up the *H wall*, a density increase at the heliopause. The H wall has been predicted by *Baranov et al.* [1991] and confirmed by various observations [e.g. *Lallement et al.*, 1993; *Linsky and Wood*, 1996; *Gloeckler et al.*, 1997]. At the termination shock, the number density of the secondary neutrals is comparable to the number density of the primary interstellar atoms (Figure 2A, dashed curve). The relative abundances of PIAs and HIAs entering the heliosphere depends on the degree of ionization in the interstellar medium. It has been shown by *Izmodenov et al.* [1999] that the relative abundance of HIAs inside the termination shock increases with increasing interstellar proton number density. The bulk velocity of HIAs is about 18-19 km/s. This population approaches the Sun. The velocity distribution of HIAs is not Maxwellian. The velocity distributions of different populations of H atoms were calculated in *Izmodenov et al.* [2001] for different directions from upwind. The fine structures of the velocity distribution of the primary and secondary interstellar populations vary with direction. These variations of the velocity distributions reflect the geometrical pattern of the heliospheric interface. The velocity distributions of the interstellar atoms can provide good diagnostics of the global structure of the heliospheric interface.

The third component of the heliospheric neutrals, **HSWAs**, corresponds to **the neutrals created in the heliosheath** from hot and compressed solar wind protons. The number density of this population is an order of magnitude smaller than the number densities of the primary and secondary interstellar atoms. This population is of minor importance for interpretations of Ly α and pickup ion measurements inside the heliosphere. However, some of these atoms may probably be detected by Lyα hydrogen cell experiments due to their large Doppler shifts. Due to their high energies, the particles influence the plasma distributions in the LIC. Inside the termination shock the atoms propagate freely. Thus, these atoms can be the source of information on the plasma properties in the place of their birth, i.e. the heliosheath.

The last population of heliospheric atoms is SSWAs, **the atoms created in the supersonic solar wind**. The number density of this atom population has a maximum at $\sim$5 AU from the sun. At this distance, the number density of population 1 is about two orders of magnitude smaller than the number density of the interstellar atoms. Outside the termination shock the density decreases faster than $1/r^2$ where r is the heliocentric distance (curve 1, Figure 2B). The mean velocity of population 1 is about 450 km/sec, which corresponds to the bulk velocity of the supersonic solar wind. The *supersonic* atom population results in the plasma heating and deceleration upstream of the bow shock. This leads to the decrease of the Mach number ahead of the bow shock.

SSWAs velocities are Doppler shifted out of the solar H Lyman α line and therefore are not detectable by interplanetary Lyman α measurements. Atoms of the three other populations penetrate the heliosphere and may backscatter solar Lyα photons. This is in contrast to the classical hot model [*Thomas*, 1978; *Lallement et al.*, 1985] which assumed that at large heliocentric distance the velocity distribution is Maxwellian and unperturbed by the heliospheric interface interaction.

In what follows, we will use these three populations to compute the interplanetary UV background. Each population will be referred to by use of its label (PIA, HIA, HSWA). The hydrogen distribution model will be called the three population model, noted $3p$ model, because the SSWA is invisible to Lyα light.

3. Radiative transfer model

The LISM neutral hydrogen gas is without any doubt an optically thick medium for solar Lyman α photons at the large heliocentric

Table 1. The P10 data, position and solar flux

Year	Day	heliocentric distance (AU)	ecliptic latitude of P10 measured from Earth	ecliptic longitude of P10 measured from Earth	Solar Lyman α flux (photons/ cm2/s)	counts per sec
1979	298	20.0043	3.257	59.982	5.7e11	405.30
1980	252	22.5058	3.325	62.662	5.4e11	362.66
1981	207	25.0001	3.347	64.615	5.19e11	323.33
1982	167	27.5037	2.561	65.600	5.05e11	268.33
1983	129	30.0002	2.589	65.772	5.10e11	214.90
1984	95	32.5061	3.308	66.293	4.71e11	185.57
1985	61	35.0067	3.030	67.902	3.89e11	149.01
1986	30	37.5069	2.380	68.560	3.52e11	128.23
1987	1	40.0006	2.842	69.712	3.72e11	135.35
1987	338	42.5012	2.628	71.280	4.01e11	145.84
1988	314	45.0111	2.544	72.150	5.03e11	169.28

Table 2. Sets of model parameters and results

Model	$n_{H,LIC}$	$n_{p,LIC}$	sqrt(Least squares sum)	Calibration factor
1	0.15	0.07	40.9	2.04
2	0.2	0.05	71.8	3.16
3	0.2	0.10	50.7	2.26
4	0.2	0.20	50.4	1.80
5	0.25	0.10	56.9	3.08

distances considered here. This is because the scattering path length for neutral hydrogen density of 0.1 cm^{-3} will be of the order of 10 to 15 AU. This implies that the radiative transfer calculation of Lyman α photons at heliocentric distances greater than 15 AU must necessarily take into account multiple scattering. In fact, a full treatment of the solar Lyman α radiative transfer problem must include the actual self-reversed solar line shape, multiple scattering, full angular and frequency redistribution function, Doppler and aberration effects, heliosphere-wide hydrogen temperature and velocity changes and Voigt Lyman α absorption profile.

The Monte Carlo radiative transfer calculation performed here is a revised version of the code published in *Gangopadhyay, Ogawa and Judge* [1989]. The original 1989 code agreed with *Keller et al.* [1981] for a hot hydrogen model. The 1989 code included a flat solar line, multiple scattering, complete frequency redistribution, constant hydrogen temperature and Doppler absorption profile. The 1989 model has now been completely revised to incorporate all the requirements listed in the previous paragraph.

The radiative transfer code is outlined below:

1. The hydrogen Ly α photons are launched from the sun, which is the origin of the coordinate system.

2. The direction of launch is determined randomly. θ is the angle between the launch direction and the upwind direction and ϕ is the azimuth angle around the interstellar flow direction which is the line of symmetry. The angles θ and ϕ are determined from the equations $cos(\theta) = 2t - 1$ and $\phi = 2\pi t$, respectively, and t is a random number between 0 and 1.

3. The photon frequency is determined by inverting the solar Lyman α profile [*Lemaire et al.*, 1978].

4. The optical depth of the photon is given by $\tau = -ln(t)$. The new position of the photon is found by inverting the optical depth.

5. It is checked whether the photon entered the field of view of a UV detector with a specific look angle.

6. The photon is followed till it crosses a cut-off optical depth of 75. Then a new photon is followed by going to step 1.

7. As long as the photon optical depth is less than the cut-off optical depth, the photon is scattered again. Gamma, the scattering angle is obtained from the relation:

$$cos(\gamma) = (t - 0.5)\frac{24}{11} - (t - 0.5)^3\frac{8}{11}$$

The azimuth angle ϕ around the incident direction is given by $\phi = 2\pi t$.

8. The new frequency ν_p is obtained by inverting the redistribution function [*Mihalas*, 1978]:

$$R(\nu, \nu_p) = \frac{g}{\pi sin\theta} exp[-\frac{1}{2}(x - x')^2 cosec^2\frac{\theta}{2}] \times H(asec\frac{\theta}{2}, \frac{1}{2}(x + x')sec\frac{\theta}{2}), \quad (1)$$

where g is the angular phase function. $x = (\nu - \nu_0)$/(Doppler width) and $x' = (\nu' - \nu_0)$/(Doppler width) are dimensionless frequencies of the incident and scattered photon, where ν_0 is the line center frequency. θ is the angle between the incident and scattered direction. H is the Voigt function and a is equal to $(\gamma/4\pi)$/(Doppler width) where γ is the radiative damping width of the upper state. This redistribution function is more general than other redistribution functions, like complete frequency redistribution function, commonly in use. The Mihalas redistribution function is the correct function to handle the resonant scattering of the strongly self-reversed solar line in the interplanetary medium since this function simulates nearly complete redistribution in the line core and becomes nearly coherent in the line wings [Mihalas, 1978]. Since the photon frequency and direction are calculated in the stationary sun centered frame while the hydrogen atoms have a flow velocity relative to the stationary frame, it is necessary to calculate the frequency and incident photon direction in the moving atom frame. The equations used to carry out this transformation for bulk velocity significantly less than the speed of light c are given below:

$$\frac{sin\theta' cos\phi'}{\lambda'} = \frac{sin\theta cos\phi - v_x/c}{\lambda}$$
$$\frac{sin\theta' sin\phi'}{\lambda'} = \frac{sin\theta sin\phi - v_y/c}{\lambda} \quad (2)$$

$$\frac{cos\theta'}{\lambda'} = \frac{cos\theta - v_z/c}{\lambda}$$
$$\nu' = \nu(1 - \frac{(\vec{v}\cdot\vec{k})}{c})$$

The moving atom frame is the primed frame. $\vec{k}$ is the photon direction vector and λ is the photon wavelength in the rest frame.

9. A new optical depth and a new position is chosen exactly as in step 4.

10. The code goes to step 5 and the subsequent steps are repeated.

11. The intensity in Rayleighs is calculated using the following expression:

$$4\pi I = \frac{4\pi N}{A\Omega}\frac{F_e \cdot 4\pi r_e^2}{N_{tot}}10^{-6}, \quad (3)$$

where I is the specific intensity, N is the number of photons collected in the collection area A, Ω is the solid angle of the collection cone, F_e is the integrated solar Lyman α flux at 1 AU in photons/cm^2/s, r_e is 1 AU and N_{tot} is the number of photons launched. The Pioneer 10 collection geometry, a 1^o conical ring pointing anti sunwards and centered 160^o with respect to the spacecraft spin axis pointed approximately towards the sun, was not simulated. A 5^o conical ring was used to improve the statistics. In fact, the spacecraft spin axis is supposed to point towards the Earth. However, the spin axis does drift away from the Earth and has to be occasionally corrected. The angle, Earth-spacecraft-spin axis is not allowed to exceed 0.5 degrees. Of course, for the heliocentric distances considered here, the spin axis may be thought of as pointing approximately towards the sun. The solid angle, Ω, is given by, $\Omega = 2 * \pi * (cos(17.5) - cos(22.5))$, where 22.5 and 17.5 are the semi vertex angles of the outer and inner collection cones. The photons are collected on a 20 degree wide patch of the collection sphere centered at the sun of radius equal to the heliocentric distance [*Gangopadhyay, Ogawa and Judge*, 1989]. The error (rayleighs) is calculated by dividing the intensity (Rayleighs) by the square root of the number of photons collected.

4. Pioneer 10 instrumentation and data

The Ultraviolet photometers on-board Pioneer 10 cover two broad spectral regions. The long wavelength channel is sensitive to emissions shortwards of 1400 A, which includes the Ly α emission line. The short wavelength channel is sensitive shortward of 800 A. The details of the UV photometers and their sensitivity curves are given in *Carlson and Judge* [1974].

The trajectory of Pioneer 10 lies nearly in the ecliptic and is in the downstream direction relative to the interstellar wind velocity. The details of the trajectory are given in *Wu et al.* [1988]. The detector look angle traces out a conical shell (apex angle 40 degrees and shell thickness = 1 degree) about the spacecraft spin axis. The Pioneer 10 photometer suffered a gain loss at heliocentric distances greater than about 45 AU, increasing the uncertainty from 5 % [*Wu et al.*, 1988] for data within about 45 AU of the Sun to uncertainty values still under review. The reasons for the gain loss are discussed in *Hall et al.* [1993].

We have used daily averaged Pioneer 10 Ly α data obtained at heliocentric distances between 20 and 45 AU in the present work. The inner distance limit, 20 AU, was chosen because our radiative transfer code does not generate good statistics for data positions too close to the sun. The outer limit was set at 45 AU because Pioneer 10 EUV data uncertainty increases sharply beyond 45 AU. The P10 data, position and solar flux are given in Table 1. The look angle can be calculated from the spacecraft position. For all the eleven data points, the Earth-spacecraft vector looks away from the galactic center making an angle of about 109 degrees with respect to the Galactic North pole. The count rates are converted to Rayleighs by subtracting the dead count (3 counts per sec) and dividing by 4.9. Later on we will see that the P10 intensity values obtained by this procedure need to be revised upwards. A point that needs to be made here is that our data set and the P10 data published by *Scherer and Scherer* [2001] are obtained from the same set of raw data. Any difference in the two data sets would be due to different processing of the raw data in the post 45 AU data set where P10 hydrogen channel suffered a gain loss. The difference between the data sets is insignificant for the pre 45 AU region.

5. Methodology of comparison of theory and observations

Monte Carlo radiative transfer calculations were carried out for a number of neutral hydrogen density models (Table 2). The calculated results, Icalc, were then compared with P10 EUV data (figs 4,5,6,7 and 8). In order to properly compare the data with the calculated results, it was necessary to calculate the optimum P10 instrument calibration factor (CF) for each of the density models. This step is necessary since it is known that the P10 and V1/2 instrumental calibrations differ by a factor of 4.4 at Lyman α [Shemansky et al. 1984]. The difference between the P10 photometer and V2 spectrometer calibration factors forces one to reproduce the distance dependence of the data rather than rely on the absolute value of the measured intensity. It should be stated here that the P10 photometer calibration did not drift with time during the period 1979-1988 considered here. The degradation of the P10 Bendix channel multipliers has been studied in the laboratory [*Carlson and Judge*, 1974]. It has been found that the electron multipliers can deliver about 16 coulombs of charge without any sign of fatigue. The P10 electron multiplier for the hydrogen channel is estimated to have delivered at most 4 coulombs of charge by 1988. The early degradation observed in the hydrogen channel of the P11 instrument is attributed to damage due to the hostile environment encountered by P11 during its flyby past Saturn. The optimum calibration factor for a density model is calculated by minimizing the least squares sum, LSS, where LSS is calculated by the following equation

$$LSS = \sum (I_{model} + bg - CF * I_{P10data})^2, \quad (4)$$

where summation is over the P10 data points and bg is the Lyman α galactic background. Both CF and bg were varied to obtain the minimum LSS. Once the optimum CF and bg are found then P10 data are multiplied by CF and compared with the calculated intensity. Both CF and LSS for each of the 5 density models are given in Table 2.

It is clear from Table 2 and the figures that the model with the VLISM neutral hydrogen density of 0.15 cm^{-3} and proton density of 0.07 cm^{-3} yields the lowest LSS and so best reproduces the P10 data. The next best fit occurs for the model with neutral hydrogen density of 0.2 cm^{-3} and proton density of 0.2 cm^{-3}. It is not at present possible to choose between the two neutral densities used in these two models as it is necessary to calculate model results for other ionization ratios for both of these cases and compare with P10 data. The Lyman α background, bg, was determined to be negligibly small for all the density models. In fact the best fit was obtained for bg equal to zero although the deviation of the data from the best fit curve (Figure 4) was from + 22 to - 16 Rayleighs. The background glow is assumed to be approximately the same for all eleven data points since the look directions are approximately the same with respect to the galactic plane. A look at Table 2 and the figures also show that the largest deviation from the P10 data occurs for the

model in which neutral density is 0.2 cm^{-3} and proton density=0.05 cm^{-3}. The ionization ratio ($n_p/(n_H+n_p)$) for this model is 0.2.

The value 0.2 might well be the lower limit of the LISM ionization ratio. This is because the LISM neutral hydrogen density can not be too high because of the growing evidence that the neutral hydrogen density inside the termination shock is of the order of 0.1 cm^{-3} or less. For example, *Wang and Richardson* [2001] suggest that the Voyager 2 solar wind observations are best fitted with an interstellar neutral hydrogen density of 0.08 cm^{-3} at the termination shock. Such a low neutral hydrogen density at the termination shock would imply a neutral hydrogen density of 0.16 cm^{-3} at "infinity" even assuming that the neutral hydrogen suffers a 50 % depletion at the interface. Similarly, *Gloeckler and Geiss* [2001] found that the neutral hydrogen density at the termination shock is 0.115 cm^{-3} and obtained a value of 0.18 cm^{-3} for the interstellar hydrogen density assuming a 58 % filtration effect. We did not use a very high interstellar neutral hydrogen density as that will imply a large neutral density inside the heliosphere which would contradict observational evidence [*Gloeckler and Geiss*, 2001; *Wang and Richardson*, 2001].

It is possible to estimate the upper limit to the ionization ratio from the fact that the model with neutral and proton densities equal to 0.2 cm^{-3} (ionization ratio =0.5) gives better fit to the Pioneer 10 data than the models discussed previously except for the first model in Table 2. However, such a high proton density is ruled out as it would imply a solar wind shock too close to the sun contrary to observations. Thus, an ionization ratio as high as 0.5 would imply a low neutral density and a ratio higher than 0.5 is extremely unlikely. The relatively high value of the ionization ratio (0.2 to 0.5) estimated in this work clearly shows that the VLISM neutral hydrogen density can not be as high as 0.25 cm^{-3}. This is because it is clear from figure 8 and from the better fit obtained for the model with both proton and neutral densities equal to 0.2 cm^{-3} that an ionization

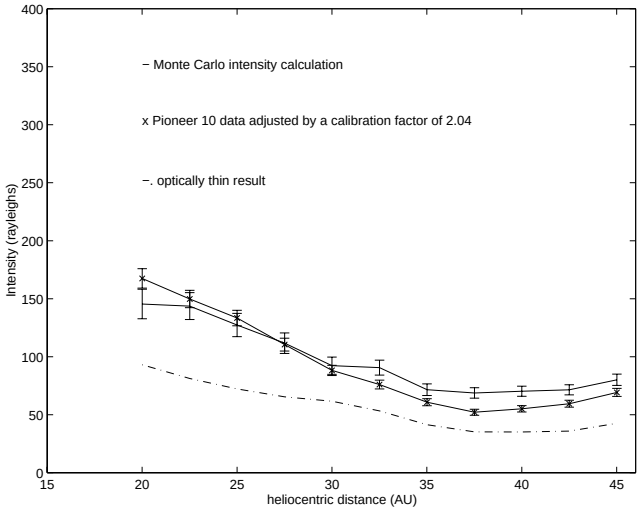

Figure 4. Comparison of Monte Carlo optically thick and optically thin calculations using heliospheric model with neutral hydrogen density of 0.15 cm^{-3} and proton density of 0.07 $^{-3}$ and Pioneer 10 Lyman Alpha glow data adjusted by the constant calibration factor as function of heliocentric distance.

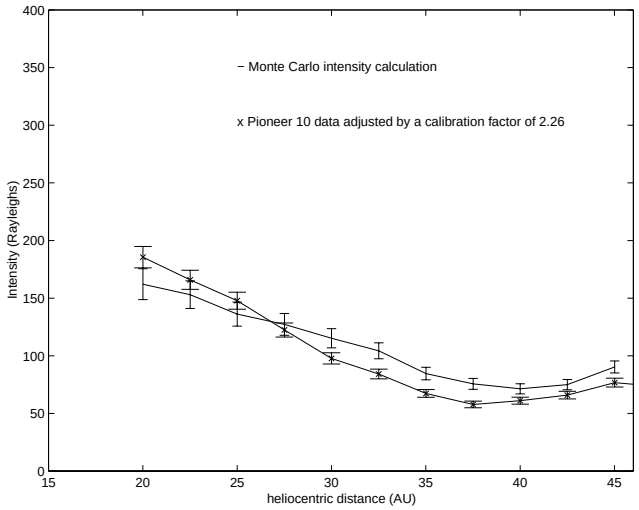

Figure 6. Same as in figure 4 except that a heliospheric model with neutral hydrogen density of 0.2 cm^{-3} and proton density of 0.1 cm^{-3} was used

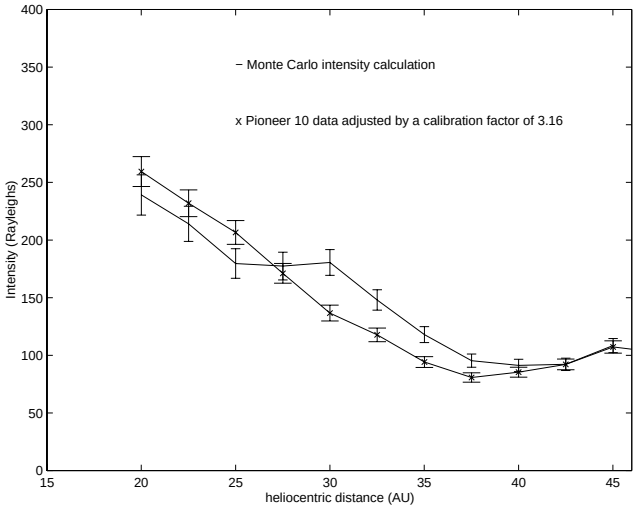

Figure 5. Same as figure 4 except that a heliospheric model with neutral hydrogen density of 0.2 cm^{-3} and proton density of 0.05 cm^{-3} was used

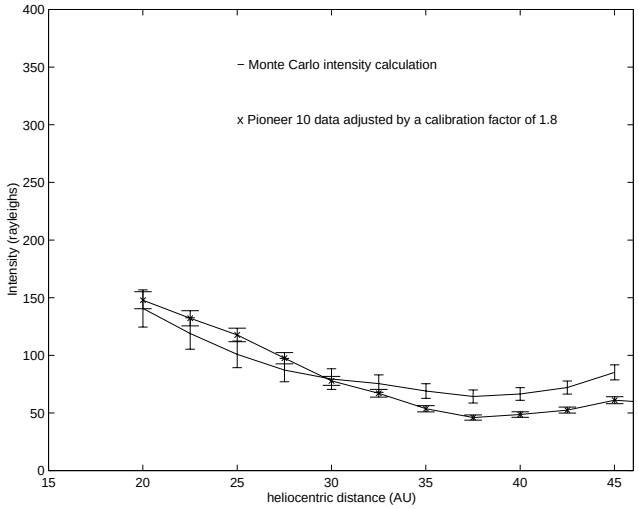

Figure 7. Same as in figure 4 except that a heliospheric model with neutral hydrogen density of 0.2 cm^{-3} and proton density of 0.2 cm^{-3} was used

ratio substantially higher than 0.3 would be necessary to better fit the neutral density, 0.25 cm^{-3}, model with the P10 data. However, even an ionization ratio of 0.4 for a neutral hydrogen density of 0.25 cm^{-3} would imply a proton density of about 0.18 cm^{-3} which would move the solar wind termination shock too close to the sun.

Another issue that needs to be discussed is the possible reasons for the deviation of the model calculation from the P10 data. The obvious reason is, of course, the difference of the model neutral hydrogen density from the actual heliospheric neutral density. Another reason is the possible variation of the solar Lyman α line center flux with respect to the integrated line [*Lemaire et al.*, 1998]. We have plotted the ratio of the model intensity to the P10 data against solar Lyman α flux in order to see if the deviation is due to the variation in line center flux. There is a trend for the ratio to decline from greater than 1 to less than 1 as the solar flux increases. This trend might be due to the line center flux variation.

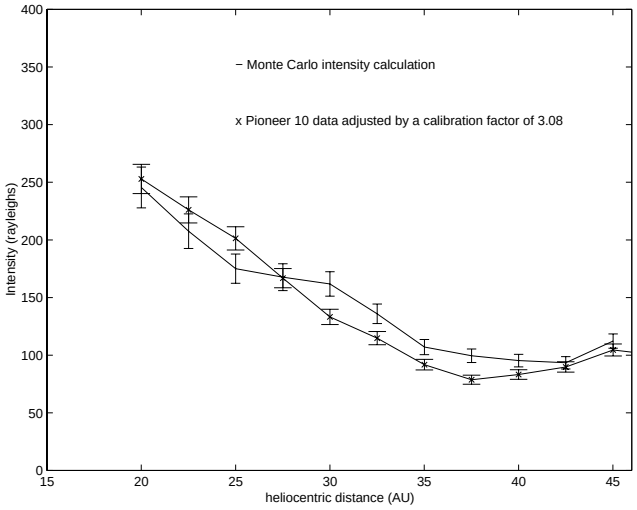

Figure 8. Same as in figure 4 except that a heliospheric model with neutral hydrogen density of 0.25 cm^{-3} and proton density of 0.1 cm^{-3} was used

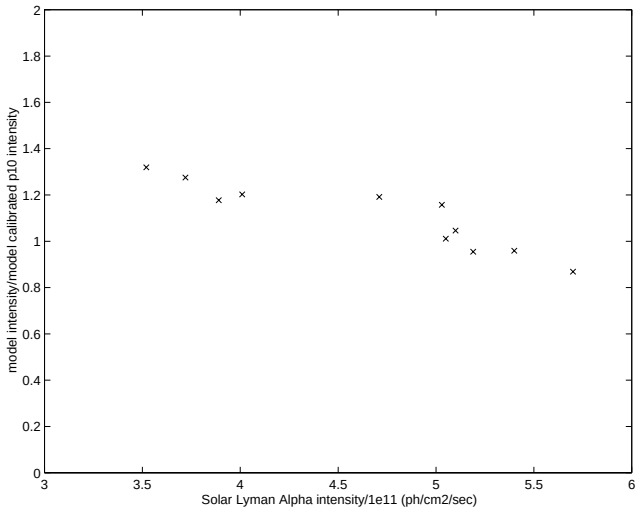

Figure 9. The ratio of the model intensity to the model calibrated P10 data as function of the solar Lyman α flux. The model intensities are for the best fit heliospheric model with neutral hydrogen density 0.15 cm^{-3} and proton density 0.07 cm^{-3}.

Figure 4 also shows a comparison between optically thick and optically thin radiative transfer calculations. The difference is significant. This is a direct confirmation that the interstellar gas is optically thick medium and does not support the recent claims of Scherer and Fahr, 1996, Scherer, Fahr and Clarke, 1997 and Scherer et al. 1997 that the gas is optically thin.

6. Conclusion

The comparison of predicted Lyman α glow using state of the art heliosphere model and Monte Carlo radiative transfer calculations with P10 data has yielded several constraints on the VLISM parameters. The ionization ratio is found to vary between 0.2 and 0.5. The upper limit to the neutral hydrogen density is found to be less than 0.25 cm^{-3}. The optimum calibration factor was found to vary from 1.8 to 3.2 for the five models used in this work. The calibration factor is found to be 2 for the model (neutral density =0.15 cm^{-3}; proton density = 0.07 cm^{-3}) that best fit the data. This work suggests that P10 UV photometer flux data values need to be increased by a factor of 2. There is some evidence that solar line center flux variation will have to be taken into account in the interpretation of the P10 data.

Acknowledgments. This work was supported by NASA grant NAG5-10989. V.I. was also supported in part by CRDF Award RP1-2248, INTAS 2001-0270, INTAS YSF 00-163, RFBR grants 01-02-17551, 02-02-06011, 01-01-00759, and International Space Science Institute in Bern.

References

Ajello, J.M., Stewart, A. I., Thomas, G. E., Graps, A., Solar cycle study of interplanetary Lyman α variations - Pioneer Venus Orbiter sky background results, Astrophysical Journal, 1, 317, 964-986. 1987.

Axford, W.I., The interaction of the solar wind with the interstellar medium, in Solar Wind, NASA Spec. Publ., NASA SP-308, 609, 1972.

Baranov, V. B., Lebedev, M. G., Malama, . G., The influence of the interface between the heliosphere and the local interstellar medium on the penetration of the H atoms to the solar system, *Astrophys. J.*, 375, 347-351, 1991.

Baranov, V. B., Malama, Y. G., Model of the solar wind interaction with the local interstellar medium - Numerical solution of self-consistent problem, *J. Geophys. Res.* 98, pp. 15,157-15,163, 1993.

Baranov, V. B., Malama, Y. G., Effect of local interstellar medium hydrogen fractional ionization on the distant solar wind and interface region,*J. Geophys. Res.* 100, pp. 14,755-14,762, 1995.

Baranov, V. B., Malama, Y. G., Axisymmetric Self-Consistent Model of the Solar Wind Interaction with the Lism: Basic Results and Possible Ways of Development *Space Sci. Rev.* 78,Issue 1/2, p. 305-316, 1996.

Baranov, V. B., Izmodenov, V. V., Y. G., On the distribution function of H atoms in the problem of the solar wind interaction with the local interstellar medium, *J. Geophys. Res.* 103, 9575-9586,1998.

Cummings, A.C., Stone, E.C., and Webber, Estimate of the distance of the solar wind termination shock from gradients of anomalous cosmic ray oxygen, J. Geophys. Res., 98, 15,165, 1993.

Gangopadhyay, P., Ogawa, H. S., Judge, D. L., Evidence of a nearby solar wind shock as obtained from distant Pioneer 10 ultraviolet glow data, *Astrophys. J.*, , 336, 1012-1021, 1989.

Gangopadhyay, P. and Judge, D.L., UV remote detection of the solar wind termination shock, *Advances in Space Research*, 15, 8/9, 463-466, 1995.

Gangopadhyay, P. and Judge, D. L., Model-insensitive and Calibration-independent Method for Determination of the Downstream Neutral Hydrogen Density Through Lyman α Glow Observations, *Astrophys. J.*, , 467, 865-869, 1996.

Gloeckler, G., Geiss, J., Fisk, L., Anomalously small magnetic field in the local interstellar cloud, *Nature* 386, 374-377, 1997.

Gloeckler, G. and Geiss, J., Heliospheric and Interstellar phenomena deduced from pickup ion observations, Space Science Reviews, 97, 1/4, 169, 2001.

Hall, D.T., Shemansky, D.E., Judge, D.L., Gangopadhyay, P., Gruntman, M.A., Heliospheric hydrogen beyond 15 AU: evidence for a termination shock, *J. Geophys. Res.*, 98, 15,185 - 15, 192, 1993.

Holzer, T.E., Interaction of the solar wind with the neutral component of the interstellar gas, J. Geophys. Res., 77, 5407, 1972.

Izmodenov, V. V., Physics and Gasdynamics of the Heliospheric Interface, *Astrophys. Space Sci.* 274, 55-69, 2000.

Izmodenov, V. V., Lallement, R., a, Yu. G., Heliospheric and it astrospheric hydrogen absorption towards Sirius: no need for interstellar hot gas, A&A 342, L13-L16, 1999.

Izmodenov, V. V., Gruntman, M., , Yu. G., Interstellar hydrogen atom distribution function in the outer heliosphere, *J. Geophys. Res.* 106, 10681-10690, 2001.

Keller, H.U., Richter, K., and Thomas, G.E., Multiple scattering of solar resonance radiation in the nearby interstellar medium II, Astron Astrophys, 102,415, 1981.

Kurth, W.S. and Gurnett, D.A., Plasma waves as indicators of the termination shock, J. Geophys. Res., 98, 9, 1993.

Lallement, R., Bertaux, J.L., and Clarke, ., Deceleration of Interstellar Hydrogen at the heliospheric interface, Science, 260, 1095, May 21, 1993.

Lemaire, P., Charra, J., Jouchoux, A., Vidal-Madjar, A., Artzner, G.E., Vial, J.C., Bonnet, R.M., Skumanich, A., Calibrated full disk solar HI Lyman α and Lyman $beta$ profiles, *Astrophys. J.*, , 223, L55, 1978.

Lemaire, P., Emerich, C., Curdt, W., Schuhle, ., and Wilhelm, K., Solar HI Lyman α full disk profile obtained with OHO spectrometer, Astron Astrophys, 334, 1095, 1998.

Linsky, J.L., Wood, B.E., The A lpha Centauri line of sight: D/H ratio, physical properties of local interstellar gas, and measurement of heated hydrogen ("The Hydrogen Wall") near the heliopause, The Astrophys. J, 463, 254, 1996.

Malama, Y. G.,Monte-Carlo simulation of atoms trajectories in the solar system, *Astrophys. Space Sci.* 176, 21-46, 1991.

Mihalas, D., Stellar Atmospheres, W.H. Freeman and company, 1978.

Quémerais, E., Bertaux, J.-L., Sandel, B., Lallement, R., A new measurement of the interplanetary hydrogen density with ALAE/ATLAS 1,*Astronomy and Astrophysics*, 290, 941-955, 1994.

Quémerais, E., Sandel, B. R., Lallement, R., Bertaux, J.-L., A new source of Ly α emission detected by Voyager UVS: heliospheric or galactic origin, *Astronomy and Astrophysics*, 299, 249-257, 1995.

Quémerais, E.,Malama, Y. G., Sandel, W. R., Lallement, R., Bertaux, J.-L., Baranov, V. B., Outer heliosphere Lyman α background derived from two-shock model hydrogen distributions: application to the Voyager UVS data, *Astronomy and Astrophysics*, 308, 279-289, 1996.

Scherer, H., and Fahr, H.J., Lyman α transport in the heliosphere based on an expansion into scattering hierarchies, Astron. Asyrophys., 309, 957, 1996.

Scherer, H., and Scherer,K., New results derived from Pioneer 10/11 UV data, in Proceedings of COSPAR Colloquium on The Outer Heliosphere: The Next Frontiers, 137-149, 2001.

Scherer, H., Fahr, H.J., and Clarke, J.T., Analysis of interplanetary H-Ly Alpha spectra obtained with the telescope GHRS spectrometer, Astron. Astrophys., 325, 745, 1997.

Scherer, H., Bzowski, M., Fahr, H.J., and Rucinski, D., Improved analysis of interplanetary HST-H Lyman Alpha spectra using e-dependent modelings, Astron. Astrophys., 342, 601, 1999.

Shemansky, D. E., Judge, D. L., Jessen, J. M., Pioneer 10 and Voyager observations of the interstellar medium in scattered emission of the He 584 A and H Lyα 1216 A lines In NASA. Goddard Space Flight Center Local Interstellar Medium, No. 81, 24-27, 1984.

Tobiska, W. K., Pryor, W. R., Ajello, J. M., Solar hydrogen Lyman α variation during solar cycles 21 and 22,*Geophys . Res. Lett.*, 24, 1123-1127, 1997.

Wang, C., and Richardson, J.D., Energy Partition between solar wind protons and pickup ions in the distant heliosphere: A three-fluid approach, J. Geophys.Res. 106, 29401, 2001.

Witte, M., Rosenbauer, H., Banaszkiewicz, M., r, H., The ULYSSES neutral gas experiment - Determination of the velocity and temperature of the interstellar neutral helium, *Advances in Space Research*, vol. 13, no. 6, p. 121-130, 1993.

Witte, M., Banaszkiewicz, M., Rosenbauer, H., cent Results on the Parameters of the Interstellar Helium from the Ulysses/Gas Experiment, 1996, *Space Science Reviews* 78, Issue 1/2, p. 289-296.

Woods,T.N. and Rottman, G.J., Solar Lyman α irradiance measurements during two solar cycles, *J. Geophys. Res.*, 102,8769-8779, 1997.

Woods,T.N., Tobiska, W.K., Rottman, G.J., and 'Worden, J.R., Improved solar Lyman α irradiance modeling from 1947 through 1999 based on UARS observation, *J. Geophys. Res.*, 105,27,195-27,215, 2000.

Wu, F.M., Judge,D.L., Suzuki, K., Carlson, R.W., Pioneer 10 ultraviolet photometer observations of the interplanetary glow at heliocentric distances from 2 to 14 AU, *Astrophys. J.*, , 245, 1145-1158, 1981.

Wu, F.M., Gangopadhyay, P., Ogawa, H.S., Judge, D.L., The hydrogen density of the local interstellar medium ultraviolet observations, *Astrophys. J.*, , 331, 1004-1012, 1988.

P Gangopadhyay,University of Southern California, Los Angeles (pradip@lism.usc.edu)

Vlad Izmodenov, Lomonosov Moscow State University, Department of Aeromechanics and Gas Dynamics, Faculty of Mechanics and Mathematics, Moscow, 119899, Russia (izmod@ipmnet.ru)

(Received February 23, 2002; accepted 1.)